Electronic Supplementary Material (ESI) for Nanoscale.

Supporting Information for

High-Performance p-i-n Perovskite Photodetectors and Image Sensors with Long-Term Operational Stability Enabled by a Corrosion-Resistant Titanium Nitride Back Electrode

Tian Sun[1], Tong Chen[1], Jiahao Chen[1], Qiang Lou [1], Zihao Liang[1], Guijun Li[2], Xiaoyun Lin[1], Guoshen Yang[1], Hang Zhou[1]**

1. School of Electronic and Computer Engineering, Peking University Shenzhen Graduate School, Shenzhen 518055, China

2. Key Laboratory of Optoelectronic Devices and Systems of Ministry of Education and Guangdong Province, College of Physics and Optoelectronic Engineering, Shenzhen University

*Corresponding author: gliad@connect.ust.hk; zhouh81@pkusz.edu.cn.

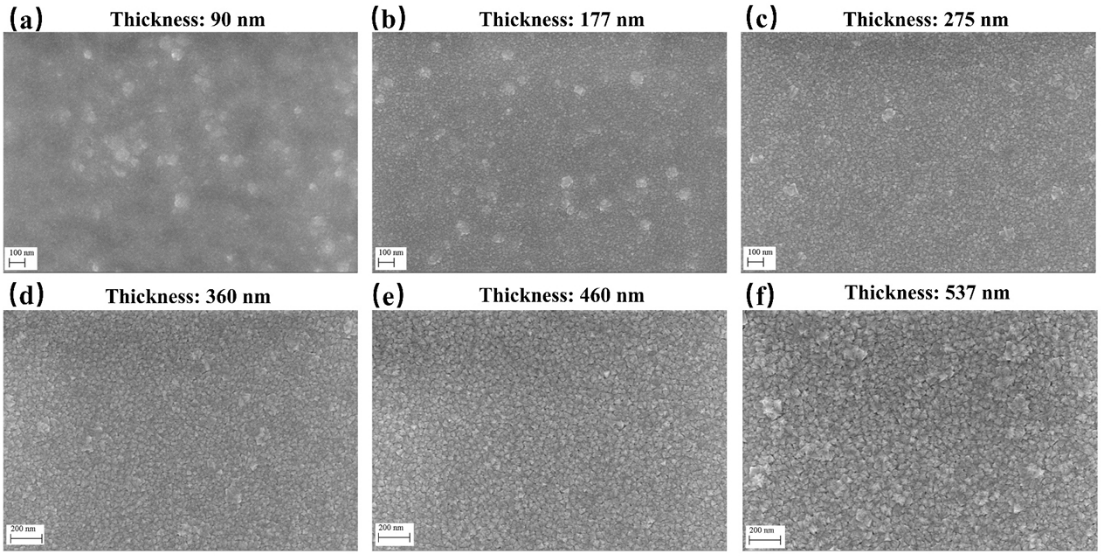

Figure S1. The top-view of TiN films sputtered on C_{60} with different thicknesses (a) 90 nm (b) 177 nm (c) 275 nm (d) 360 nm (e) 460 nm (f) 537 nm

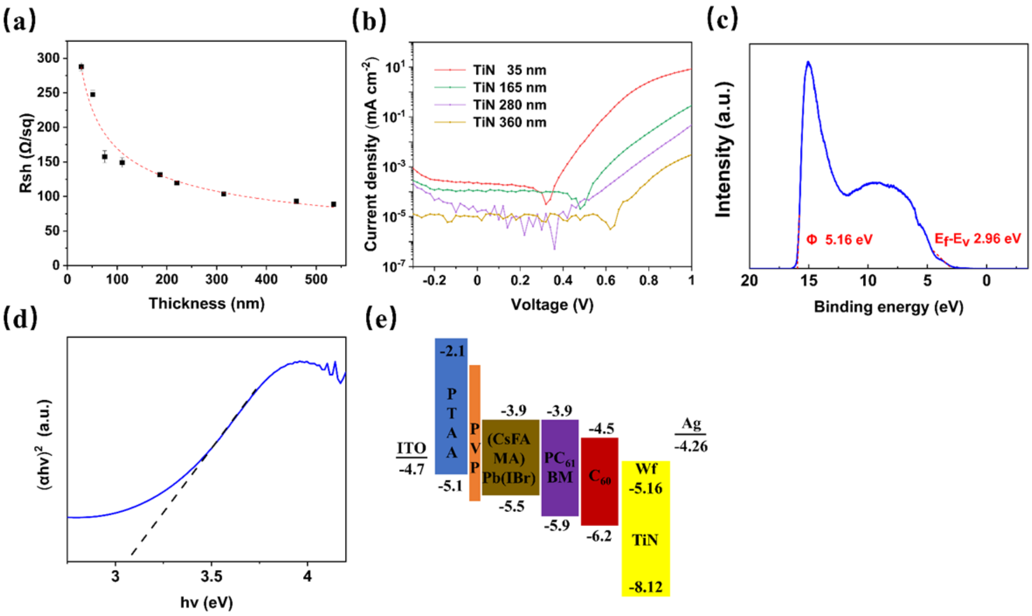

Figure S2. (a) R_{sh} as a Function of Thickness of TiN Films (b) The dark current of TiN-based perovskite photodiode with different TiN thickness (c) The UPS spectrum of TiN film using He I excitation (21.2 eV) (d) The Plot of $(\alpha h\nu)^2$ against photon energy for the TiN thin film, which indicates a direct bandgap of ~3.06 eV (e) Energy level of the TiN-based photodetector.

Table S1 Simulation parameters of TiN-based perovskite photodetector for energy band in this study.

	PTAA	Perovskite	PCBM	C_{60}	TiN
Eg(eV)	3[1]	1.6[2]	2.0[3]	1.7[4]	3.06
χ (eV)	2.1[1]	3.9[2]	3.9[3]	4.5[4]	5.06
Thickness (nm)	20	600	40	20	360
N_A(cm^{-3})	1e18	0	0	0	0
N_D (cm^{-3})	0	0	2.93e17[5]	2e18[4]	2.5e20
N_C(cm^{-3})	2e18[6]	2.5e20[7]	2.5e21[8]	2.2e18[4]	2.5e21
N_V(cm^{-3})	2e19[6]	2.5e20[7]	2.5e21[8]	1.8e19[4]	2.5e21

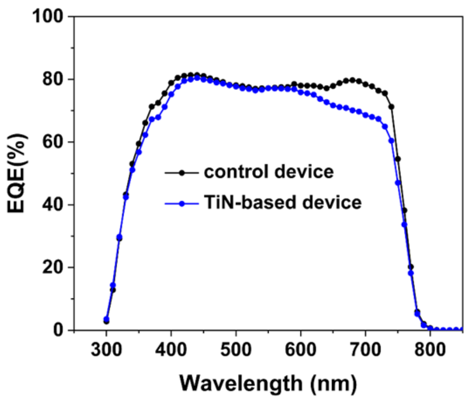

Figure S3 EQE of perovskite photodiodes with and without TiN.

Table S2 The rise time and fall time of TiN-based photodetector measured at different frequencies

Frequency (hz)		250	500	1000	2000	3000	4000
Control device	Rise time (μs)	98.4	101	103	102	88.9	77.4
	Fall time (μs)	102	101	94	103	92.6	91.5
Control device (-0.2 V)	Rise time (μs)	98.3	100	89.5	97.7	93.2	76.6
	Fall time (μs)	105	103	103	102	97.2	79.1
TiN-based device	Rise time (μs)	108	127	112	117	94.4	85.2
	Fall time (μs)	102	146	98.1	107	104	78.2
TiN-based device (-0.2 V)	Rise time (μs)	112	106	104	108	96.5	86.5
	Fall time (μs)	116	116	94.3	110	98	78.3

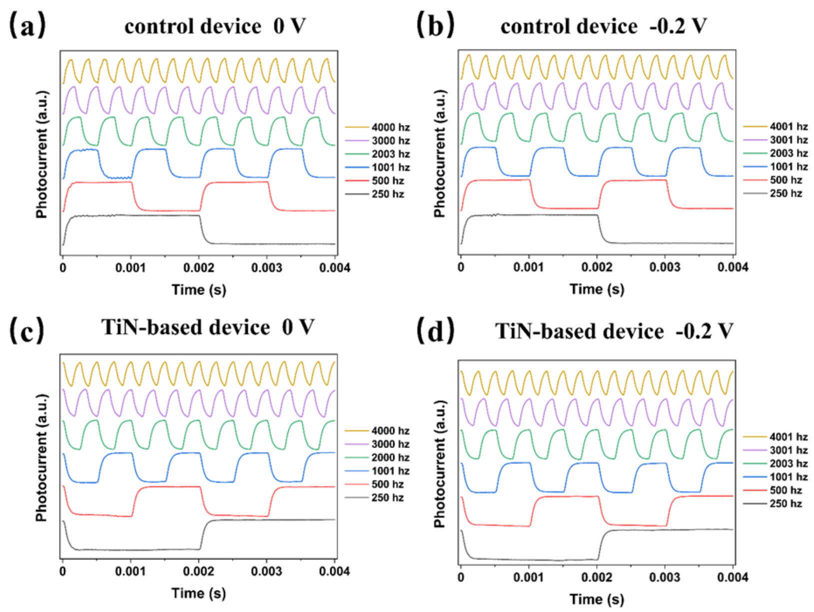

Figure S4 (a) The response of control device under 520 nm light (intensisty: 1.54 mW cm^{-2}) at different frequencies (a) under 0 bias (b) under -0.2 V bias The response of

TiN-based device under 520 nm light (intensisty: 1.54 mW cm^{-2}) at different frequencies (c) under 0 bias (d) under -0.2 V bias

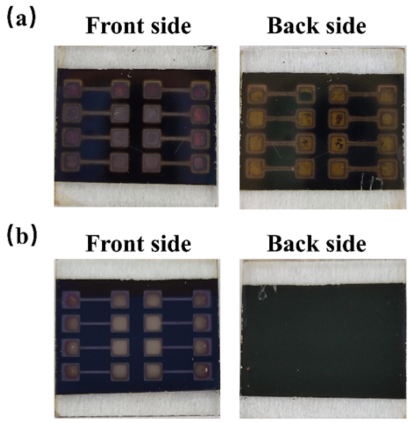

Figure S5 Appearance of electrodes aged for 507 hours at 85 °C (a) control group: photodetector without TiN (b) TiN-based photodetector

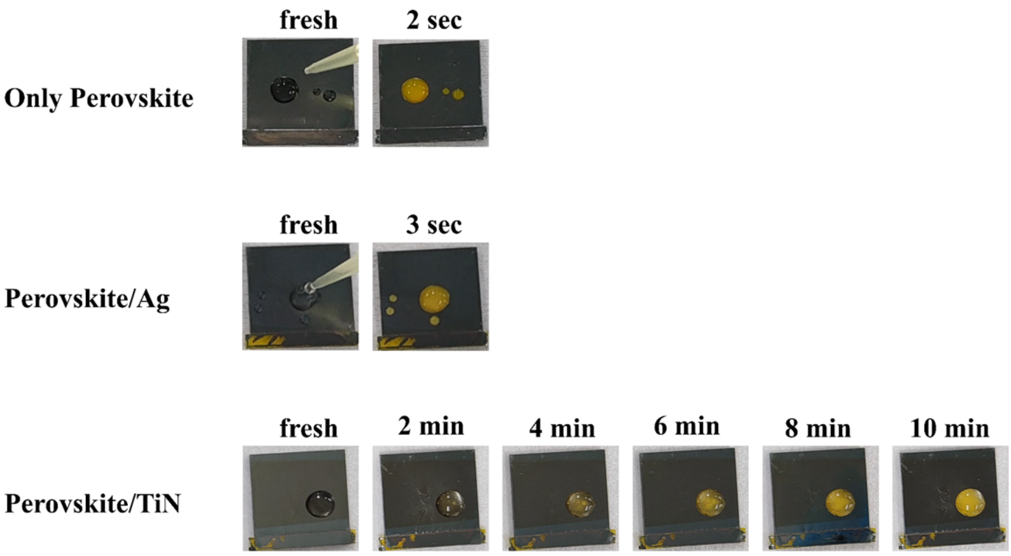

Figure S6 Dripping water of different films. Only perovskite, perovskite/Ag (10 nm), and perovskite/TiN (10 nm) films, respectively.

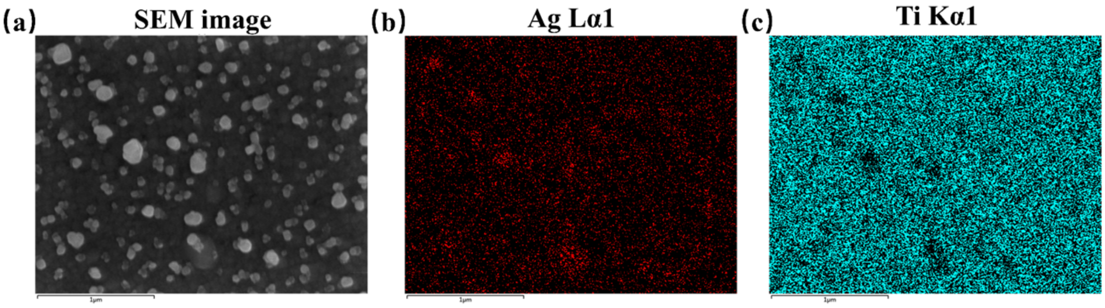

Figure S7 (a) Top-view SEM of TiN-based device (b) Ag EDS map (c) Ti EDS map

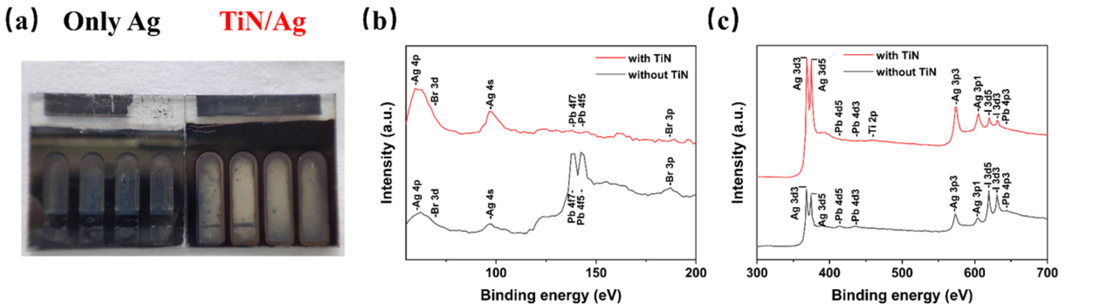

Figure S8 (a) Electrode appearance of aged device. (b-c) The XPS spectra of electrodes for control device and TiN-based device.

Table S3 The atomic content of elements estimated by XPS

Atomic concentration (%)	Without TiN	With TiN
Ag 3d (%)	56.8	87.0
I 3d (%)	38.3	9.8
Pb 4f (%)	4.9	0.2
Br 3d (%)	$<$0.1	$<$0.1
Ti 2p (%)	—	3.0
Total (%)	100	100

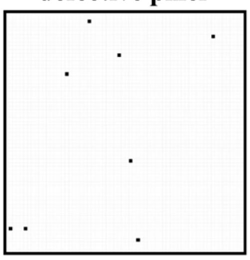

Figure S9 aged array defective spot detection (185 days with glass encapsulation)

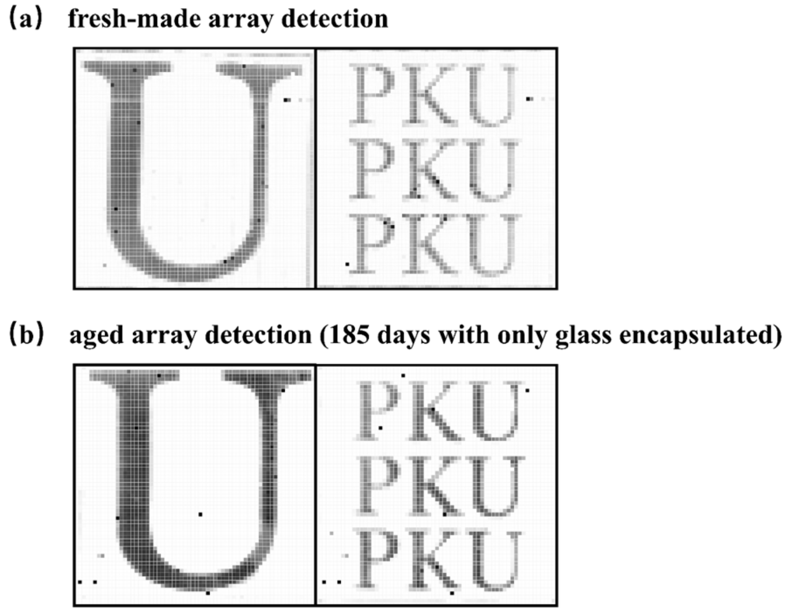

Figure S10 (a) The imaging performance for fresh-made device (b) The imaging performance for aged device. (185 days with glass encapsulation)

REFERENCES

1. J. Xu, J. Dai, H. Dong, P. Li, J. Chen, X. Zhu, Z. Wang, B. Jiao, X. Hou, J. Li and Z. Wu, *Organic Electronics*, 2022, **100**, 106378.
2. D. Luo, T. Zou, W. Yang, B. Xiang, X. Yang, Y. Wang, R. Su, L. Zhao, R. Zhu, H. Zhou, T. P. Russell, H. Yu and Z.-H. Lu, *Advanced Functional Materials*, 2020, **30**, 2001692.
3. O. Malinkiewicz, A. Yella, Y. H. Lee, G. M. Espallargas, M. Graetzel, M. K. Nazeeruddin and H. J. Bolink, *Nature Photonics*, 2014, **8**, 128-132.
4. Z. Qirong, Z. Bao, H. Yongmao, L. Liang, D. Zhuoqi, X. Zaixin and Y. Xiaobo, *Materials Research Express*, 2022, **9**, 036401.
5. S. K. Saha, A. Guchhait and A. J. Pal, *Physical Chemistry Chemical Physics*, 2012, **14**, 8090-8096.
6. D. K. Jarwal, A. K. Mishra, A. Kumar, S. Ratan, A. P. Singh, C. Kumar, B. Mukherjee and S. Jit, *Superlattices and Microstructures*, 2020, **140**, 106463.
7. W. A. Laban and L. Etgar, *Energy & Environmental Science*, 2013, **6**, 3249-3253.
8. Y. Wang, Z. Xia, J. Liang, X. Wang, Y. Liu, C. Liu, S. Zhang and H. Zhou, *Semiconductor Science and Technology*, 2015, **30**, 054004.